CO$_2$-responsive swelling behavior and metal-ion adsorption properties in novel histamine-conjugated polyaspartamide hydrogel

Ngoc Bich Tran, Jae Yun Kim, Youn-Chul Kim, Young Jun Kim, Ji-Heung Kim

Department of Chemical Engineering, Sungkyunkwan University, Jangan Suwon, South Korea
Correspondence to: J. H. Kim (E-mail: kimjh@skku.edu)

ABSTRACT: Novel polyaspartamide copolymers containing histamine pendants (PHEA-HIS) were prepared from polysuccinimide, which is the thermal polycondensation product of aspartic acid, via a successive ring-opening reaction using histamine (HIS) and ethanolamine (EA). The prepared water-soluble copolymer was then crosslinked by reacting it with hexamethylene diisocyanate in order to provide a hydrogel with both good gel strength and reversible CO$_2$ absorption characteristics. PHEA-HIS gel is also pH-sensitive and eligible to coordinate to metal ions such as Pb^{2+}, Cu^{2+}, and Ni^{2+} due to the imidazole units in its structure. The CO$_2$-responsive swelling behavior, metal-ion adsorption, and morphology of the crosslinked gels were investigated. The approach described here results is a promising hydrogel with potential for a variety of industrial and biomedical applications including CO$_2$ capture, CO$_2$-responsive and switchable sensors, and smart drug delivery systems. © 2015 Wiley Periodicals, Inc. J. Appl. Polym. Sci. **2016**, *133*, 43305.

INTRODUCTION

Stimuli-responsive smart polymers that respond in a significant way to slight external changes have attracted considerable recent attention.[1–8] These materials have been explored as carriers for controlled drug release, scaffolds for tissue engineering, actuators, and sensors in biomedical devices.[9–12] Hydrogels are hydrophilic polymer networks capable of absorbing large amounts of water, yet are insoluble due to the presence of physical or chemical crosslinks, entanglements, or crystalline regions. As a nontoxic, inexpensive, benign and abundant gas, CO$_2$ is able to reversibly switch solvent,[13,14] solutes,[15] and surfactants,[16] all of which bear amidine or guanidine functional groups. Additionally, CO$_2$ can stabilize the intracellular pH value via a series of equilibrium reactions (CO$_2$ + H$_2$O $\leftrightarrow$ H$_2$CO$_3$ $\leftrightarrow$ H$^+$ + HCO$_3^-$). Determining the construction of a CO$_2$-responsive polymer system remains a challenge, since the influence of gas on hydrogel behavior has rarely been inspected.[17]

Over the past decades, continuous increases in water pollution are closely tied to the progressive increase in industrial activities. Contamination by heavy metals has become a critical problem, as the metals accumulate over time in the environment.[18,19] Several conventional techniques have been employed to treat effluent before it is discharged into the environment, such as chemical precipitation, ion exchange, reverse osmosis, membrane separation, filtration, electrochemical treatment, and evaporative recovery.[20–24] The adsorption method has outstanding advantages and is considered the most environmentally friendly, effective, efficient, and economic method of waste purification among the various physicochemical treatment processes.[25,26]

Histamine is a well-known amidine featuring an imidazole ring that not only exhibits CO$_2$- and pH- sensitive characteristics, but also forms metal–ligand interactions with metal ions. Histamine can be found in very small amounts in ergot, and is among the products of the bacterial decomposition of histidine; this constitutes one of the methods for its production. Histamine is produced from histidine via pneunococci or *E. coli*.[27] Poly(aspartic acid) (PASP) holds promise as a water-soluble and biodegradable polymer that can be produced from the hydrolysis of poly(succinimide) (PSI).[28–30] Recent studies of amphiphilic poly(aspartic acid) derivatives have been reported by several research groups.[31–33] PASP, becoming highly absorbent when neutralized and crosslinked, is pH and electrolyte sensitive in water and body fluids.[34–37] The PSI backbone can be easily modified to form hydrophilic–hydrophobic copolymers. Polyaspartamides (PolyAspAm)s include a wide range of PASP amide derivatives that can be prepared using either an aminolysis reaction with PSI or a secondary reaction of carboxylic pendant groups of PASP. The various aminolysis reactions can then convert PSI into more useful functional polymers or crosslinked gel materials.[38–43] In this work, we report a facile and versatile strategy for the preparation of CO$_2$-responsive polymers, based on poly(2-hydroxyethyl aspartamide) modified with a histamine

unit, PHEA-HIS. This polymer was crosslinked to provide a hydrogel featuring not only reversible CO_2-responsive and pH-sensitive characteristics, but also an adsorption capacity for heavy metal ions.

EXPERIMENTAL

Materials and Instruments

L-aspartic acid ($\geq$98%), o-phosphoric acid (98%), 2-aminoethanol (EA; 99%), histamine dihydrochloride ($\geq$98%), N,N-dimethylformamide (DMF; anhydrous 99.8%), dimethyl sulfoxide (DMSO, $\geq$99.7%), hexamethylene diisocyanate (HMDI; 98%), triethylamine (TEA, $\geq$99.5%) were purchased from Aldrich Chemical and used as received. All other chemicals purchased were of quality sufficient for use without purification. ^{1}H NMR spectra were recorded on a Bruker AMX-500 spectrometer using D_2O as the solvent. A small amount of the dry gels were milled into powder with KBr to prepare thin pellet. The FT-IR spectra were obtained using attenuated total reflection (ATR FT-IR) spectroscopy (Bruker IFS 66/S, Germany). The morphology of the freeze-dried gel was observed using field emission scanning electron microscopy (FE-SEM, JEOL 6320, Japan). The swollen gels were quickly quenched and then cross-sectioned in liquid nitrogen. Porous gel samples were mounted onto a metal stub with double-sided carbon tape and coated with platinum for 30 s under vacuum (10^{-3} torr) using a plasma sputtering method (HC-21 ion sputter coater). The concentration of Cu(II) and Ni(II) were determined via a flame atomic adsorption spectrometer (AAS; Buck Scientific 210VGP, USA).

Solubility Measurement

Measurement of the solubility behavior of PHEA-HIS was conducted in mixtures of distilled water and isopropanol (IPA) with various ratios. Nearly 30 mg of PHEA-HIS was completely dissolved in distilled water, IPA was then added to the polymer solution with the following IPA to H_2O ratios 1:1 (A), 1.3:1 (B), 1.5:1 (C), and 1.8:1 (D). The total volume of the four mixtures was 10 mL, and the ambient temperature was 20°C. Both the solubility and reversible behavior of the solution was monitored upon the introduction of CO_2 and N_2 into the solution. The pH values of the mixture were recorded at various points.

Swelling Capacity Measurement

The swelling ratios of the prepared gels were measured via the tea bag method. An accurately weighed portion of the powdered gel was put into a weighed tea-bag and immersed in 200 mL of distilled water at a specific temperature. The swelling ratio (SR) is defined as follows:

$$SR = \frac{W_s - W_D}{W_D},$$

where W_D and W_s are the weights of the dry and swollen hydrogels at equilibrium, respectively. Preweighed pieces of dry gel were immersed into an aqueous medium and allowed to swell. Samples of the swelled gel were removed from the solution at regular time intervals. The excess water was wiped off the surface of the gel specimens with moistened filter paper and the weights of the gels were recorded. To test the effects of CO_2, PHEA-HIS hydrogels were placed in aqueous solutions using the tea-bag method to measure the changes in hydrogel volume transition when introducing CO_2 into the solution, and are compared to the non CO_2 solution. The switching state of the PHEA-HIS hydrogel was also examined repeatedly between the carbon dioxide and nitrogen treatment for a specific period of time. The swelling degree of the hydrogels was recorded in various pH conditions, presenting the pH-stimulation of the gels.

Batch Adsorption Study

Batch adsorption studies for Cu^{2+} and Ni^{2+} ions were carried out via equilibrium experiments using copper sulfate pentahydrate and nickel sulfate hexahydrate, respectively. $CuSO_4 \cdot 5H_2O$ in various amounts was dissolved in 50 mL of deionized water. The solution was divided into 40 mL of adsorbing solution and 10 mL of initial solution. Twenty milligrams of the dry gel was added into a vial containing 40 mL of the Cu^{2+} metal ion solution. Similar experiments were performed with nickel. During the process, the original dry gels with off-white color turned into transparent light blue in copper solution and light green in nickel solution, respectively, upon swelling. After hours, the adsorption of the gels was calculated from the difference in concentration between the initial and final Cu(II) and Ni(II) solution, which was prepared by diluting 1 mL initial and terminal Cu(II) and Ni(II) solution in 99 mL of deionized water. Measurements were conducted using an AAS. The volume of deionized water was measured precisely with a 25-mL burette. The pH of the solution was controlled with HCl (0.1 N and 0.01 N) and NaOH (0.05 N) solutions. The adsorption capacity was calculated based on the difference in the initial and equilibrium metal concentrations in aqueous solution, the volume of aqueous solution (40 mL), and the weight of the adsorbent (20 mg) according to the equation below:

$$q(\text{mg/g}) = \left(C_{in} - C_{eq}\right)\frac{V}{m}, \tag{1}$$

where C_{in} is the initial metal concentration (ppm), C_{eq} is the equilibrium metal concentration (ppm), V is the volume of the metal solution (ml), and m is the weight of the dry gel adsorbent.

Synthesis of Polysuccinimide (PSI)

L-aspartic acid (20 g) and o-phosphoric acid (20 g) were poured into a round-bottom flask and stirred under reduced pressure at 180°C for 5 h. The reaction mixture was then cooled and DMF was added to dissolve the product. The resulting solution was precipitated in excess water and the precipitate was washed several times with water to remove residual phosphoric acid. The final product was dried at 80°C under vacuum. The molecular weight was estimated to be ~130,000 Da, as calculated from an empirical equation relating the solution viscosity to the molecular weight.[28]

Synthesis of PHEA-HIS

PSI (0.5 g) was dissolved in 15 mL of DMSO in a three-neck round-bottom flask equipped with a nitrogen inlet and outlet. Histamine dihydrochloride (50 mol %, based on succinimide unit) and 1.8 mL Et$_3$N were mixed in a vial before addition to the polymer solution. The reacting solution was heated to 70°C and stirred for 4 days. The polymer was then cooled to room temperature followed by the addition of an excess amount of EA and stirred for 1 day. The final solution was dialyzed for days to remove the remaining solvent before freeze-drying in vacuum (yield = 80–85%).
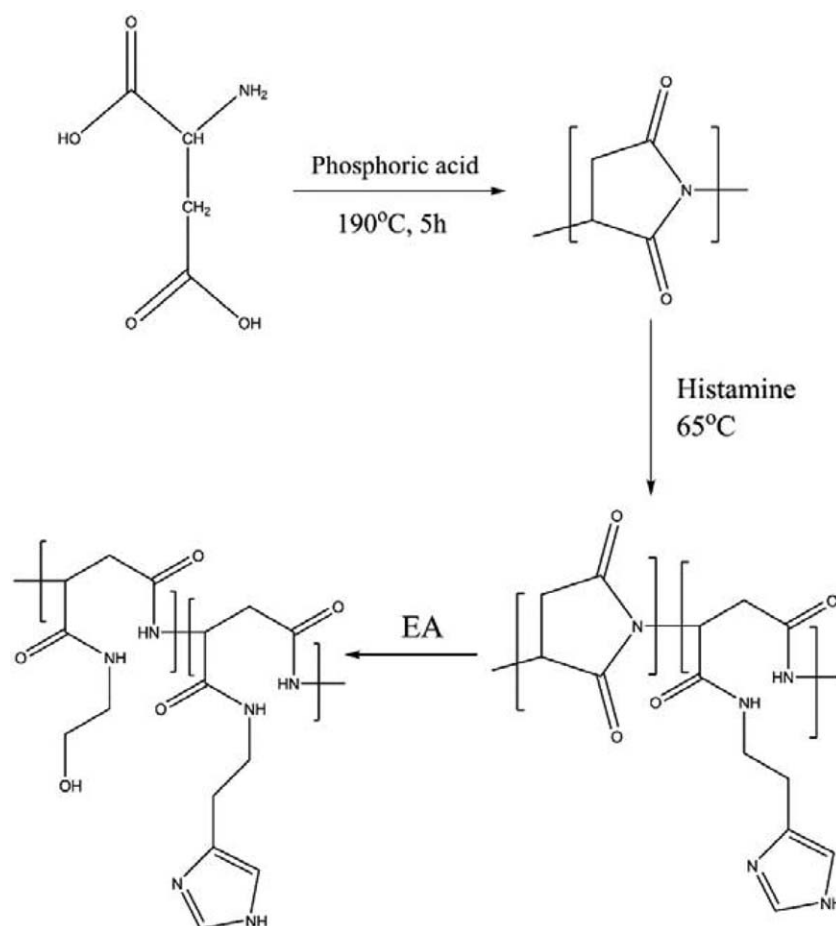
Scheme 1. The synthesis route of PHEA-HIS.

Preparation of PHEA-HIS Crosslinked Hydrogels

Crosslinked gel was prepared using the following procedure: 10 w/v % PHEA-HIS (0.2 g) was dissolved in a vial containing DMSO. Subsequently, 20 mol % HMDI (based on the hydroxyl groups in the structure), was added and stirred continuously at room temperature. The resulting PHEA-HIS crosslinked gel was formed after 2 h and then placed in a closed steel mesh and washed with a large amount of distilled water, which was changed frequently for 1 day to completely remove the unreacted components and DMSO. Finally, the washed gel product was freeze-dried in vacuum for 3 days. In this study the hydrogel sample was freeze-dried in order not to change the structure of original swollen gel and also to provide a porous gel network.

RESULTS AND DISCUSSION

Characterization of PHEA-HIS

The synthesis of PSI, the precursor polymer, has been well described in the literature.[44] A polyaspartamide derivative containing histamine pendants (PHEA-HIS) was synthesized from PSI via successive nucleophilic ring-opening reactions using histamine and ethanolamine (Scheme 1). Figure 1 shows the ^{1}H NMR spectrum of PHEA-HIS. The methylene proton peaks, E and F, appearing in the PHEA-HIS spectra were assigned to the pendent hydroxyethyl. Peaks A and B were assigned to the two heteroaromatic proton singlets of the imidazole ring. The two

peaks C and D were assigned to the two methylene protons of the histamine group. The composition of each group in PHEA-HIS was determined from the integration ratio between D
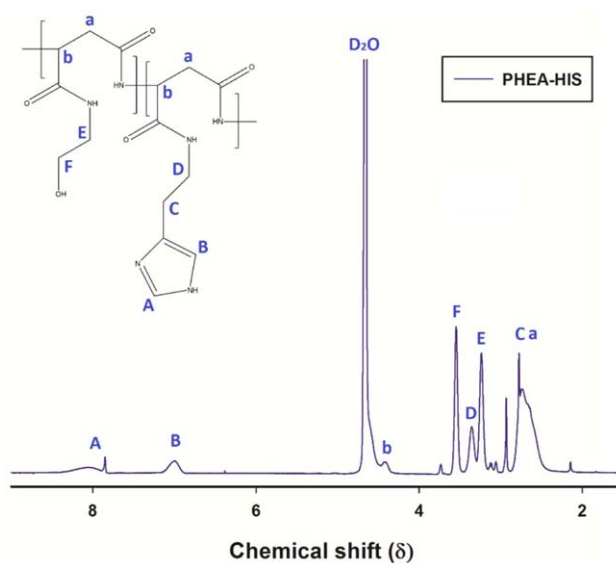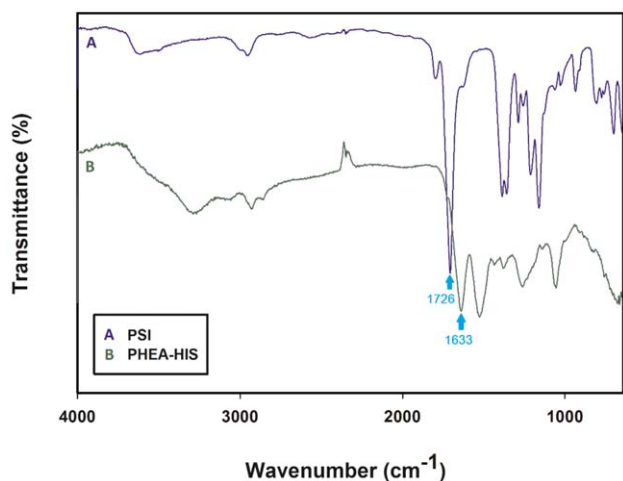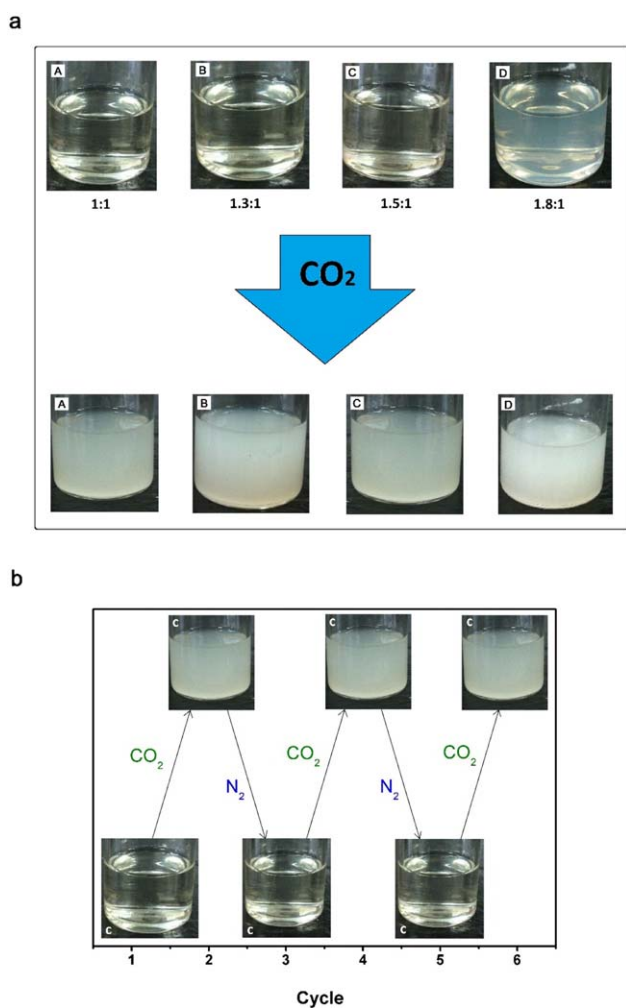

Figure 1. ^{1}H NMR of PHEA-HIS. [Color figure can be viewed in the online issue, which is available at wileyonlinelibrary.com.]
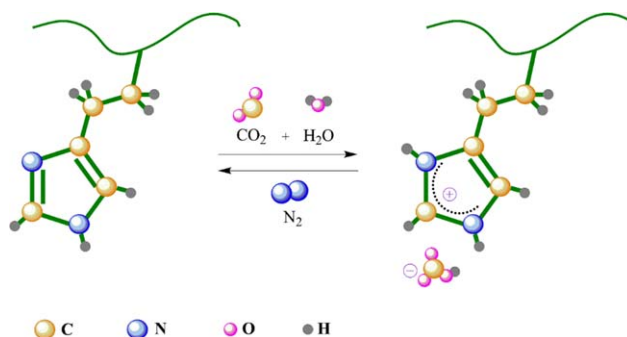
Figure 2. FTIR of PHEA-HIS. [Color figure can be viewed in the online issue, which is available at wileyonlinelibrary.com.]

($\delta = 3.28$–3.45) and E ($\delta = 3.15$–3.28). The histamine group was conjugated into the polymer backbone around 30.3%.


Figure 3. Solubility behavior of PHEA-HIS. [Color figure can be viewed in the online issue, which is available at wileyonlinelibrary.com.]


Scheme 2. CO_2 absorption via the imidazole group of histamine in the presence of water. [Color figure can be viewed in the online issue, which is available at wileyonlinelibrary.com.]

Figure 2 describes the FTIR spectra of PSI and PHEA-HIS. The PSI spectrum exhibits a characteristic strong band at 1726 cm^{-1} (absorption of imide), and this band disappears in spectrum B of the PHEA-HIS. In spectrum B, strong bands appear at around 1633 cm^{-1} (the C=O stretch of amide and C=N stretching mode of the ring, including conjugated C=C) and 1256 cm^{-1} (C—H (ring) in-plane bending and C—N (ring) stretching modes). The absorption band at about 1522 cm^{-1} was assigned to the NH stretch of amide, corresponding to the aspartamide back-bone structure. A strong band can also be observed at nearly 1061 cm^{-1}, indicating a C—N bond in the histamine. The broad band of spectra B in the range 3500–3200 cm^{-1} is attributed to the —OH of the copolymer.

Solubility Behavior of PHEA-HIS. The solubility of the PHEA-HIS polymer is illustrated in Figure 3. As shown in Figure 3(a), the higher mixed solvent ratio of 1.8:1 (IPA:water) began to turn the solution turbid, but is worth noting that IPA is not a solvent for this polymer. Bubbling CO_2 into all four solutions caused them to change from transparent to opaque (A–C), and even the heterogeneous solution D, became more turbid. By bubbling CO_2 into water, the histamine groups of PHEA-HIS will be protonated, making the solubility of the polymer more
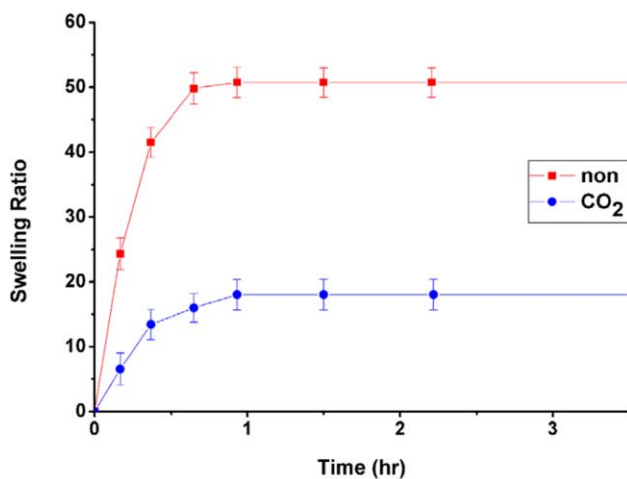
Figure 4. Swelling ratio of PHEA-HIS gel with and without CO_2. [Color figure can be viewed in the online issue, which is available at wileyonlinelibrary.com.]
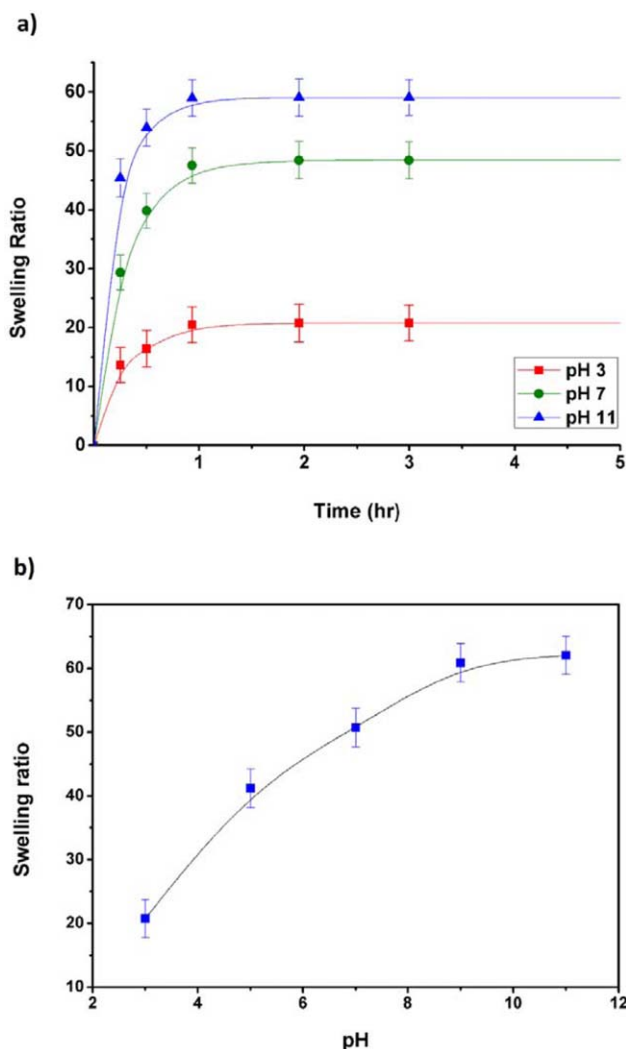
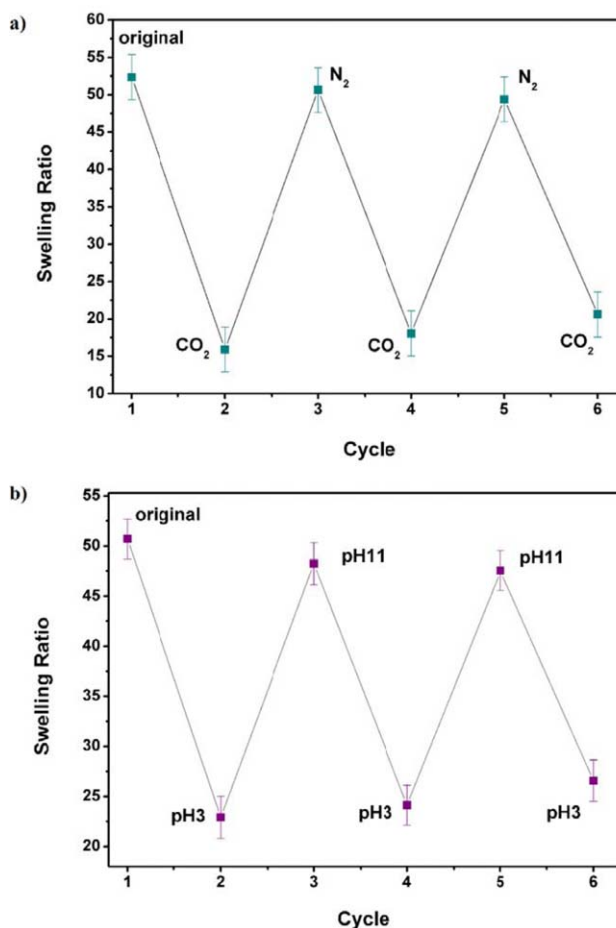**Figure 5.** Swelling ratio of PHEA-HIS gel in various pH environments. [Color figure can be viewed in the online issue, which is available at wileyonlinelibrary.com.]

prepared under various conditions. Swelling was equilibrated in about 1 h. The swelling degree of the PHEA-HIS gel, originally about SR $\sim$50 g g^{-1}, decreased noticeably to SR $\sim$18 g g^{-1} when CO_2 was bubbled into the solution containing the gel specimen. The imidazole ring of the histamine group, acting as a "proton bank," accepting protons on its free base form and donating them when it is protonated, is an amphoteric compound. When CO_2 gas is bubbled into the water, carbonic acid (H_2CO_3) is formed and the pH of the solution drops to $\sim$3.35. Similar to the effect of CO_2 on the solubility of PHEA-HIS, described previously, the gel in the CO_2 bubbled solution seemed to become more hydrophobic, causing it to shrink. In an acid solution with pH lower than 4, imidazole moieties on the polymer pendants became protonated, and the protonation induces chain stiffness via intra/intermolecular hydrogen bonding interaction between adjacent imidazole units, consequently lowering the solvent quality of the aqueous media.[37] On the contrary, in the absence of specific, stabilizing interactions, a polymer backbone will "sample" all possible conformations randomly. The above argument can explain the unusual swelling behavior of the PHEA-HIS gel that lead to shrinkage in the hydrogel upon the bubbling of CO_2 through the solution.

unfavorable in a given solvent. Presumably a change in the polymer's conformation occurs, making the interactions between polymer and solvent more unfavorable. This would, of course, be directly related to the ability of intramolecular hydrogen bond opening to create different spatial situations.[45] Reversible switching behavior of the PHEA-HIS solution is demonstrated in Figure 3(b). After bubbling the N_2 gas, the mixture once again became transparent; this process was repeatable many times. The capture of CO_2 can easily be reversed by introducing N_2 into the system. The reversible binding of CO_2 onto the imidazole groups in the presence of water is represented in Scheme 2.

Swelling Behavior of Crosslinked Hydrogels
PHEA-HIS was crosslinked using HMDI to provide the corresponding hydrogel. The prepared gels were tested to determine their swelling ratios in aqueous solution using the tea-bag method, and the water absorption was measured as a function of time. Figure 4 presents the swelling curves of the hydrogel

Figure 6. Reversible swelling behavior: (a) in the presence of CO_2/N_2 and (b) in various pH conditions. [Color figure can be viewed in the online issue, which is available at wileyonlinelibrary.com.]
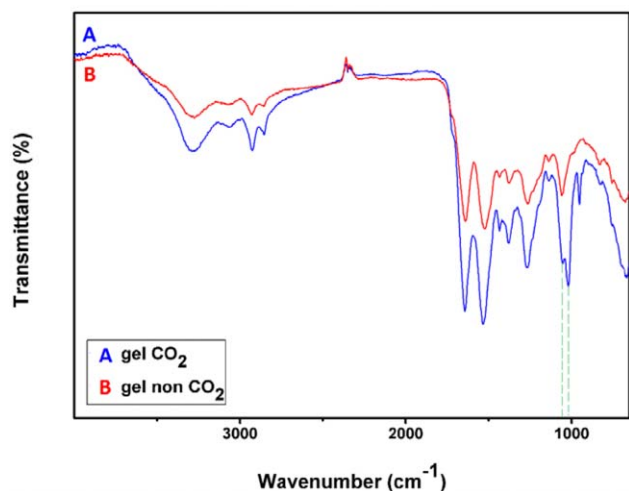
Figure 7. FTIR of PHEA-HIS hydrogel. [Color figure can be viewed in the online issue, which is available at wileyonlinelibrary.com.]

To complement the swelling behavior of the PHEA-HIS gel, the pH dependency of the solution was investigated. The swelling degree was lower at low pH and increased gradually as the increased to 8 [Figure 5(a)]. The pH-dependence of the PHEA-HIS gel is shown clearly in Figure 5(b). At pH levels of 7 and above, the hydrogel will remain practically neutral or very slightly ionized, causing the gel to expand slightly more.

Reversible Swelling of the PHEA-HIS Hydrogel

The protonation process of PHEA-HIS hydrogels can be reversed through the simple bubbling of an inert gas such as nitrogen or argon through the aqueous solution. The repeated swelling ratio changes in the presence of CO_2/N_2 and pH conditions are demonstrated in Figure 6. The pH of the solution when bubbling CO_2 was $\sim$3.35, leading to a drop in the hydrogel volume, and could be reversed to 7.56 by simply bubbling nitrogen through the aqueous solution, leading to an increase in the hydrogel volume. The reversible swelling was repeatable many times, proving that reversibility is possible in PHEA-HIS hydrogels via the introduction of CO_2/N_2 into the solution [Figure 6(a)] and controlling the pH [Figure 6(b)]. The swelling

behavior of CO_2-responsive hydrogels required less time (ca., 2 h) than responses due to pH-sensitivity (more than 4 h). Because carbon dioxide and nitrogen are both gasses at room temperature, it is easy to blow them out of the solution, while the buffer pH solution appears to take more time to affect the hydrogels. The resulting gel possesses a certain range of gel strength and degree of swelling, which is controllable by changing the concentration of either the polymer solution or cross-linker compound in the gel forming process.

IR Characterization and Morphology of the PHEA-HIS Gel

Figure 7 presents the FTIR spectra of the PHEA-HIS gels. The spectrum of the PHEA-HIS gel in non CO_2 solution shows the same peaks as the original polymer, while, in the spectrum of the CO_2-treated gel, two peaks appear at 1026 and 956 cm^{-1}, presenting the imidazole ring in its conjugate acid (imidazolium) form.

The difference in the porous structure of the two PHEA-HIS gel samples is shown in Figure 8, and agrees with the swelling behavior of the gels. In Figure 8(a), a well-interconnected microporous structure with pores 3–10 μm in size was observed, and is an effect of CO_2. The hydrogel expands to a higher swollen state in the non-CO_2 solution (see Figure 4), resulting in a macroporous structure. This change in gel porosity induced by introducing CO_2 into aqueous solution demonstrates the CO_2-based behavior of this cross-linked polymeric system.

The Swelling Properties of the Hydrogel in Various Metal Ion-containing Solutions

The swelling ratio of the hydrogel in various metal ion media indicates its fundamental adsorption capacity. Several metal ions with the same ionic numbers were used to measure the swelling degree of the hydrogel. Figure 9 shows the degree of swelling in Cu(II), Pb(II), and Ni(II) solutions compared to that in distilled water. A relatively low level of swelling in a metal-ion containing solution similar to most other known superabsorbent polymers was observed. Because of the high ionic strength, the medium acted adversely on the equilibrium swelling capacity, moreover, the multivalent coordination
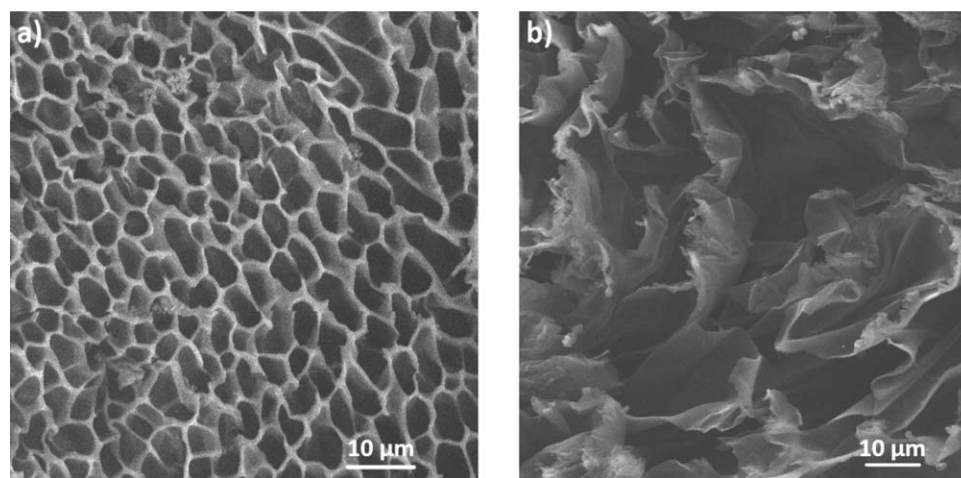
Figure 8. SEM micrographs of PHEA-HIS gel, (a) CO_2 and (b) non CO_2.
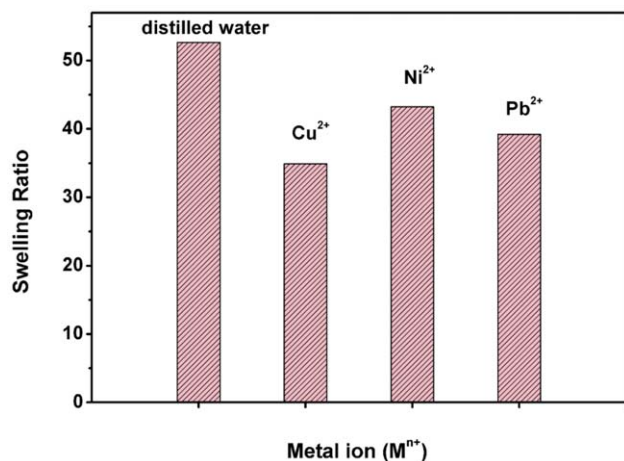
Figure 9. Swelling degree of PHEA-HIS gel in various metal ion media. [Color figure can be viewed in the online issue, which is available at wileyonlinelibrary.com.]

binding of metal-ions with imidazole groups on the polymer also lowers the swelling ratios. Here the order of swelling degree was found to be Ni(II) > Pb(II) > Cu(II).

Metal-ion Adsorption Properties

Effect of Initial Concentration and Contact Time. The amount of metal ions adsorbed onto the hydrogel at equilibrium (q_e) was studied at various initial metal ion concentrations in the range of 50–500 ppm. As shown in Figure 10, the adsorption increased from ~6–42.35 mg g^{-1} for Cu(II) and from ~27–78 mg g^{-1} for Ni(II) in aqueous solution. The adsorption of the Ni(II) ions was higher than that of the Cu(II) ions and increased more rapidly. It is believed that the adsorption of the histamine group on the nickel ion is more efficient than on other metal ions. The higher affinity of Ni(II) for imidazole renders this ligand a nickel-selective extractant,[46] however, there are fewer available sites for adsorption at high concentrations, so the adsorption of metal ions increases only slightly.[47,48]
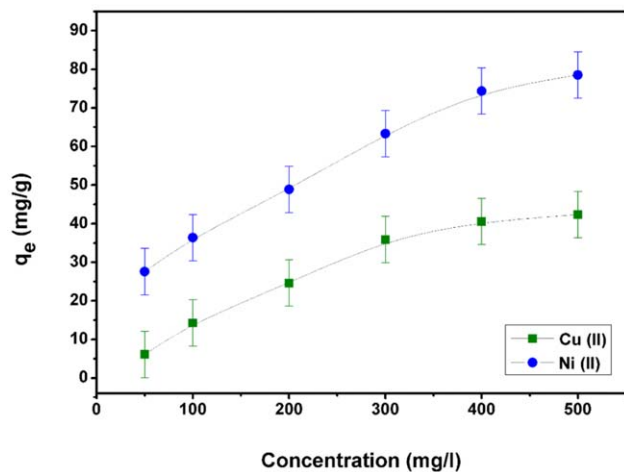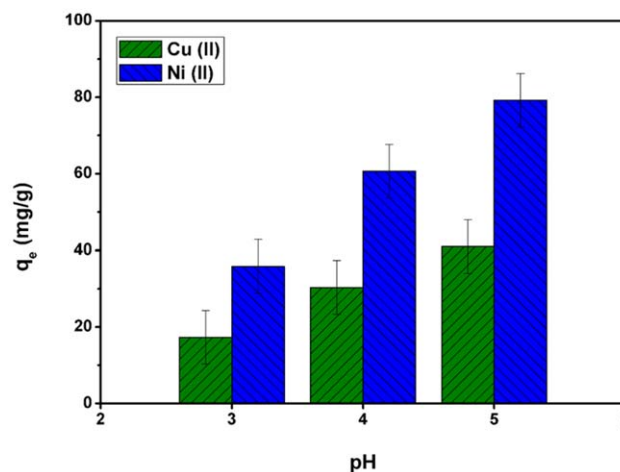

Figure 10. Effect of initial metal ion concentration on the adsorption capacity of Cu(II) and Ni(II). [Color figure can be viewed in the online issue, which is available at wileyonlinelibrary.com.]
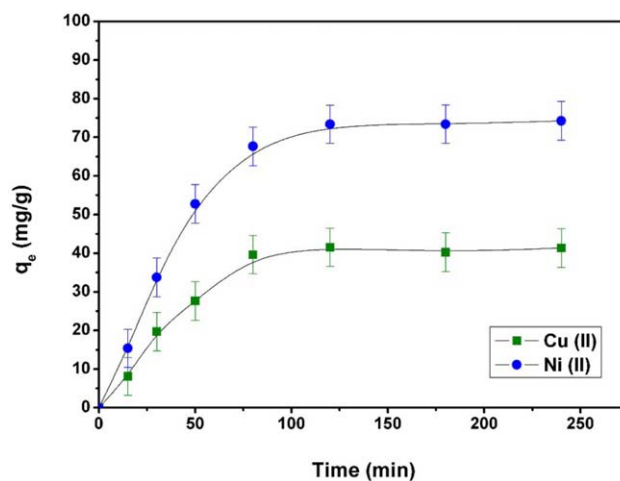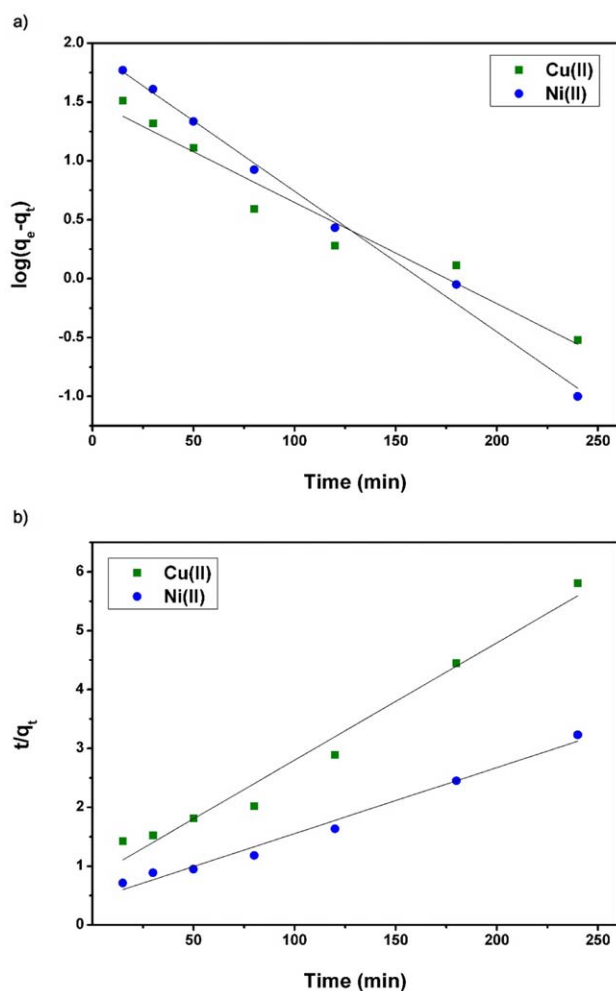

Figure 11. Effect of contact time on the adsorption capacity of Cu(II) and Ni(II). [Color figure can be viewed in the online issue, which is available at wileyonlinelibrary.com.]

The influence of time on the absorption of Cu(II) and Ni(II) ions onto hybrid gel is represented in Figure 11. The results show that the rate of adsorption of Cu(II) and Ni(II) ions is higher initially and reaches its equilibrium value after nearly 80 min for Cu(II) and 120 min for Ni(II). This is likely due to a larger surface site being available initially for the adsorption,[49] yet further increases in contact time did not offer any improvement due to rapid exhaustion of the adsorption sites after a certain contact period.[25,50]

Effect of pH on Metal Ion Adsorption. Solution pH is one of the factors that not only affects surface charge and degree of ionization, but also strongly influences the adsorption of heavy metal ions from an aqueous solution. Figure 12 describes the effect of pH on the adsorption of Cu(II) and Ni(II) from aqueous solution using PHEA-HIS gel as an adsorbent. The effect of solution pH on the Cu(II) ion and Ni(II) ion removal was investigated within the pH range of 3–5 at a metal ion

Figure 12. Effect of solution pH on the adsorption capacity of Cu(II) and Ni(II). [Color figure can be viewed in the online issue, which is available at wileyonlinelibrary.com.]

Figure 13. Pseudo-first-order (a) and pseudo-second-order (b) kinetics plot for Cu(II) and Ni(II). [Color figure can be viewed in the online issue, which is available at wileyonlinelibrary.com.]
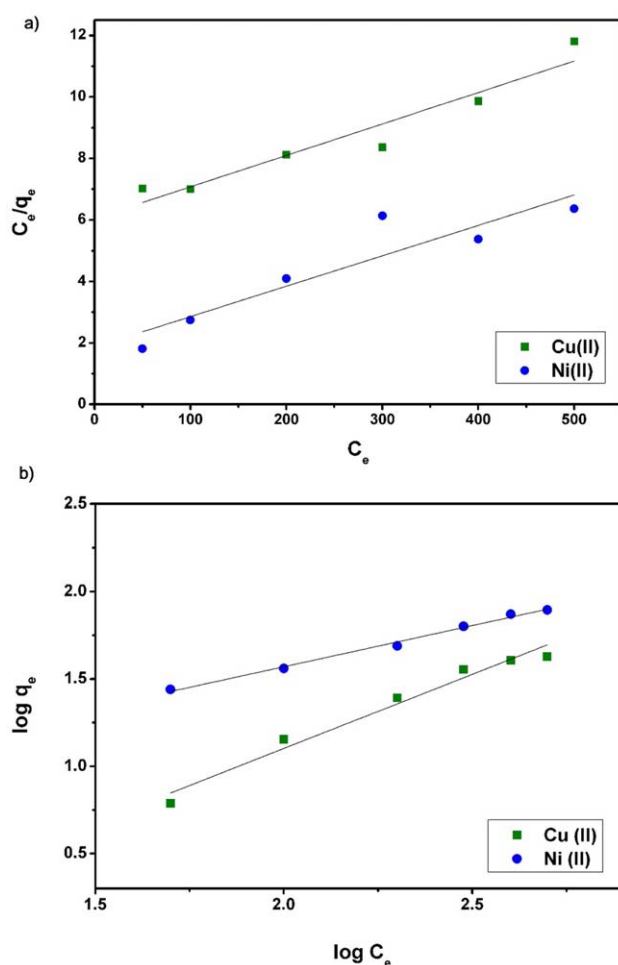
Table I. Comparison of Pseudo-First-Order and Pseudo-Second-Order Kinetics Parameters

Metal ion	Pseudo-first-order kinetic model		Pseudo-second-order kinetic model	
	k_1 (min^{-1})	R^2	k_2 (g mg^{-1} min^{-1})	R^2
Cu (II)	0.02	0.996	0.0009	0.982
Ni (II)	0.026	0.999	0.0005	0.977

$$\log(q_{e1}-q_t)=\log q_{e1}-\left(\frac{k_1}{2.303}\right)t \qquad (2)$$

$$\frac{t}{q_t}=\frac{1}{k_2\,q_{e2}^2}+\frac{t}{q_{e2}}, \qquad (3)$$

where q_{e1} (mg g^{-1}), q_{e2} (mg g^{-1}), and q_t (mg g^{-1}) are the amounts of metal ions adsorbed onto the hydrogel at equilibrium and at time, t (t is the contact time that the gels were immersed to the metal-ion containing solution). k_1 (min^{-1}) and k_2 (g mg^{-1} min^{-1}) are the pseudo-first-order rate constant and pseudo-second-order rate constant, respectively. The slopes

concentration of 400 ppm. Precipitation of the initial solution appeared at pH levels above 6. As shown in Figure 12, the adsorption capacity increased when the pH increased from pH 3–5. At low pH, the adsorption capacities of Cu(II) and Ni(II) ion were found to be lower because histamine groups in the hydrogel structure bind with specific metal ions in coordination complexes, and more H$^+$ might compete with metal ions in the adsorption sites, resulting in a decrease in divalent metal ion binding.

Adsorption Kinetics. The sorption rate is an important factor when determining the efficiency of the absorption process. The Lagergren pseudo-first-order and pseudo-second-order kinetic models are widely used to define rate of absorption from experimental data, and were used in this study to analyze the adsorption kinetics of Cu(II) and Ni(II) ions.

The linear form of the Lagergren pseudo-first-order rate equation[51] and the Morries–Weber pseudo-second-order rate equation,[52] respectively, are given as

Figure 14. Langmuir (a), and Freundlich (b) isotherm plot of the adsorption of Cu(II) and Ni(II). [Color figure can be viewed in the online issue, which is available at wileyonlinelibrary.com.]

Table II. Comparison of Langmuir and Freundlich Isotherm Parameters

Metal ion	Langmuir model			Freundlich model		
	b (L mg^{-1})	q_m (mg g^{-1})	R^2	K_f (mg g^{-1})	$1/n$ (mg mL^{-1})	R^2
Cu (II)	0.002	88	0.935	3.927	0.848	0.973
Ni (II)	0.0024	172	0.842	2.961	0.471	0.872

and intercepts of plots of log $(q_e - q_t)$ versus t were used to determine k_1 and q_{e1}, while q_{e2} and k_2 can be obtained in the same manner from the plot of t/q_t against t.

The pseudo-first-order and pseudo-second-order kinetic models were used to fit the data in Figure 11, and the results are plotted in Figure 13. The kinetic parameters obtained via the adsorption of Cu(II) and Ni(II) ions onto the PHEA-HIS hydrogel are shown in Table I. The linear correlation coefficients (R^2) of the pseudo-first-order model were higher than those of the pseudo-second-order model, and the theoretical equilibrium sorption capacity calculated from the pseudo-first-order equation was closer to the experimental sorption capacity as a function of contact time. Therefore, the linearity of these plots proves that this process follows pseudo-first-order kinetics.

Adsorption Isotherms. The adsorption capacity of the hydrogel can be illustrated via the isotherm. The equilibrium relationships between sorbent and sorbate is represented using the adsorption isotherm, which explains the adsorption behavior of solutes on adsorbents.[53] The adsorption isotherms were explored using the Langmuir[54] and Freundlich[55] adsorption models. The Langmuir model assumes a completely homogeneous adsorption surface, whereas the Freundlich isotherm is suitable for a highly heterogeneous sorption system. The two models are expressed in the following equations, respectively:

$$\frac{C_e}{q_e} = \frac{1}{bq_m} + \frac{C_e}{q_m} \tag{4}$$

$$\log q_e = \log K_f + \frac{1}{n} \log C_e, \tag{5}$$

where q_e (mg g^{-1}) is the equilibrium metal ion concentration on the sorbent, q_m (mg g^{-1}) represents the monolayer biosorption capacity of the sorbent, C_e (mg L^{-1}) is the equilibrium metal ion concentration in the solution, and b is the Langmuir adsorption constant related to the free energy of sorption. K_f and $1/n$ are the Freundlich adsorption constants indicating the adsorption capacity and adsorption intensity, respectively. The values of the Langmuir constants, b and q_m, were obtained from the slopes and intercepts of plots of C_e/q_e versus C_e, and the Freundlich constant, K_f and $1/n$, from plots of log q_e versus log C_e in the same manner.

The Langmuir and Freundlich models fitted in Figure 14 were obtained from sorbate concentration data. The constants and correlation coefficients were calculated and are shown in Table II. The linear correlation coefficients determined using the Freundlich model were greater than those of the Langmuir model, indicating that the Freundlich equation was a better fit for the experiment data than the Langmuir equation.

CONCLUSIONS

Novel polymers based on polyaspartamides with histamine functional groups and hydroxyethyl pendent groups were synthesized. Their chemical gels were prepared using HMDI in DMSO. The PHEA-HIS polymer and hydrogel are eligible for undergoing reversible switching of CO_2/N_2, which result in changes in the solubility and volume transition, respectively. The swelling and morphologies of the porous structure of the prepared gels were obtained. The hydrogels are not only CO_2-sensitive, but also respond to changes in pH, and exhibit the ability to absorb metal ions in aqueous media. The discovery demonstrated in this study opens the door to a wide range of applications including sensors, drug delivery, and even stimuli-responsive materials.

ACKNOWLEDGMENTS

REFERENCES

1. Stuart, M. A. C.; Huck, W. T. S.; Genzer, J.; Muller, M.; Ober, C.; Stamm, M.; Sukhorukov, G. B.; Szleifer, I.; Tsukruk, V. V.; Urban, M.; Winnik, F.; Zauscher, S.; Luzinov, I.; Minko, S. *Nat. Mater.* **2010**, *9*, 101.

2. Nelson, A. *Nat. Mater.* **2008**, *7*, 523.

3. Capadona, J. R.; Shanmuganathan, K.; Tyler, D. J.; Rowan, S. J.; Weder., C. *Science* **2008**, *319*, 1370.

4. Roy, D.; Cambre, J. N.; Sumerlin, B. S. *Prog. Polym. Sci.* **2010**, *35*, 278.

5. Kim, E.; Kim, D.; Jung, H.; Lee, J.; Paul, S.; Selvapalam, N.; Yang, Y.; Lim, N.; Park, C. G.; Kim, K. *Angew. Chem. Int. Ed.* **2010**, *49*, 4405.

6. Klaikherd, A.; Nagamani, C.; Thayumanavan, S. *J. Am. Chem. Soc.* **2009**, *131*, 4830.

7. Fries, K.; Samanta, S.; Orski, S.; Locklin, J. *Chem. Commun.* **2008**, *47*, 6288.

8. Nath, N.; Chilkoti, A. *Adv. Mater.* **2002**, *14*, 1243.

9. Hoffman, A. S. *Adv. Drug. Deliv. Rev.* **2002**, *43*, 3.

10. Vermonden, T.; Censi, R.; Hennink, W. E. *Chem. Rev.* **2012**, *112*, 2853.

11. Peppas, N. A.; Hilt, J. Z.; Khademhosseini, A.; Langer, R. *Adv. Mater.* **2006**, *18*, 1345.

12. Kikuchi, A.; Okano, T. *Adv. Drug Deliv. Rev.* **2002**, *54*, 53.

13. Jessop, P. G.; Heldebrant, D. J.; Li, X.; Eckert, C. A.; Liotta, C. L. *Nature* **2005**, *436*, 1102.

14. Jessop, P. G.; Phan, L.; Carrier, A.; Robinson, S.; Durr, C. J.; Harjani, J. R. *Green Chem.* **2010**, *12*, 809.

15. Phan, L.; Jessop, P. G. *Green Chem.* **2009**, *11*, 307

16. Liu, Y.; Jessop, P. G.; Cunningham, M.; Eckert, C. A.; Liotta, C. L. *Science* **2006**, *313*, 958.

17. Yan, Q.; Zhou, R.; Fu, C.; Zhang, H.; Yin, Y.; Yuan, J. *Angew. Chem. Int. Ed.* **2011**, *50*, 4923.

18. Förstner, U.; Wittmann, G. T. W. Metal Pollution in the Aquatic Environment, 2nd revised ed.; Springer Verlag: Berlin, **1983**; Vol. *18*, p 194.

19. Pehlivan, E.; Yanik, B. H.; Ahmetli, G. M.; Pehlivan, M. *Bioresour. Technol.* **2008**, *99*, 3520.

20. Akkaya, R.; Ulusoy, U. *J. Hazard. Mater.* **2008**, *151*, 380.

21. Jang, S. H.; Jeonga, G. Y.; Mina, B. G.; Lyoob, N. S.; Lee, S. C. *J. Hazard. Mater.* **2008**, *159*, 294.

22. Zhao, H.; Mitomo, H. *J. Appl. Polym. Sci.* **2008**, *110*, 1388.

23. Gavrilescu, M. *Eng. Life Sci.* **2004**, *4*, 219.

24. Reddad, Z.; Gerente, C.; Adress, I.; Cloirec, P. L. *J. Environ. Sci. Technol.* **2002**, *36*, 2067.

25. Hajeeth, T.; Vijayalakshmi, K.; Gomathi, T.; Sudla, P. *Int. J. Biol. Macromol.* **2013**, *62*, 59.

26. Zhao, G.; Wu, X.; Tan, X.; Wang, X. *Open Colloid. Sci. J.* **2011**, *4*, 19.

27. Bruhl, L. *Ann. Inst. Pasteur* **1938**, *61*, 828.

28. Neri, P.; Antoni, G.; Benvenuti, F.; Colola, F.; Gazzei, G. *J. Med. Chem.* **1972**, *16*, 893.

29. Wolk, S. K.; Swift, G.; Paik, Y. H.; Yocom, K. M.; Smith, R. L.; Simon, E. S. *Macromolecules* **1994**, *27*, 7613.

30. Nakata, T.; Yoshitake, M.; Matsubara, K.; Tomida, M.; Kakuchi, T. *Macromolecules* **1998**, *31*, 2107.

31. Moon, J. R.; Kim, B. S.; Kim, J. H. *Bull. Korean Chem. Soc.* **2006**, *27*, 981.

32. Kim, S. I.; Son, C. M.; Jeon, Y. S.; Kim, J. H. *Bull. Korean Chem. Soc.* **2009**, *30*, 3025.

33. Kim, J. H.; Son, C. M.; Jeon, Y. S.; Choe, W. S. *J. Polym. Res.* **2011**, *18*, 881.

34. Andrade, J. D. Hydrogels for Medical and Related Application, in *ACS Symp. Ser.*, No. 631, American Chemical Society: Washington DC, **1996**.

35. Min, S. K.; Kim, J. H. *Korean Polym. J.* **2001**, *9*, 143.

36. Kim, J. H.; Lee, J. H.; Yoon, S. W. *J. Ind. Eng. Chem.,* **2002**, *8*, 138.

37. Yoshimura, T.; Ochi, Y.; Fujioka, R. *Polym. Bull.,* **2005**, *55*, 377.

38. Moon, J. R.; Kim, J. H. *Polym. Int.* **2010**, *5*, 630.

39. Moon, J. R.; Kim, M. W.; Kim, D.; Jeong, J. H.; Kim, J. H. *Colloid Polym. Sci.* **2011**, *289*, 63.

40. Moon, J. R.; Jeon, Y. S.; Zrinyi, M.; Kim, J. H. *Polym. Int.* **2013**, *62*, 1218.

41. Huynh, N. T.; Jeon, Y. S.; Kim, D.; Kim, J. H. *Polymer* **2013**, *54*, 1341.

42. Giammona, G.; Pitarresi, G.; Cavallaro, G.; Carlisi, B.; Craparo, E. F.; Mandracchia, D. *J. Drug Del. Sci. Tech.* **2006**, *16*, 77.

43. Pitarresi, G.; Pierro, P.; Palumbo, F. S.; Tripodo, G.; Giammona, G. *Biomacromolecules* **2006**, *7*, 1302.

44. Kim, S. I.; Min, S. K.; Kim, J. H. *Bull. Korean Chem. Soc.* **2008**, *29*, 1887.

45. Mazurek, A. P.; Topiol, S.; Weinstein, H.; Osman, R. *Int. J. Quantum Chem.* **1983**, *24*, 293.

46. Okewole, A. I.; Antunes, E.; Nyokong, T.; Tshentu, Z. R. *Miner. Eng.* **2013**, *54*, 88.

47. Abdunnaser, M. E.; Mahmoud, E. R.; Mohamed, T. M.; Nayef, M. M. *Am. J. Anal. Chem.* **2014**, *5*, 225.

48. Liu, D.; Li, Z.; Li, W.; Zhong, Z.; Xu, J.; Ren, J.; Ma, Z. *Ind. Eng. Chem. Res.* **2103**, *52*, 11036.

49. Kumar, P. S.; Kirthika, K. *J. Eng. Sci. Technol.* **2009**, *4*, 351.

50. Oyedeji, O. A.; Osinfade, G. B. *J. Environ. Sci. Technol.* **2010**, *4*, 382.

51. Lagergren, S. *Vetenskapsakad Handl* **1898**, *24*, 1.

52. Ho, Y. S.; McKay, G.; Wase, D. A. J.; Foster, C. F. *Ads. Sci. Technol.* **2000**, *18*, 639.

53. Vadivenlan, V.; Kumar, K. V. *J. Colloid Interface Sci.* **2005**, *286*, 90.

54. Langmuir, I. *Am. J. Chem. Soc.* **1918**, *40*, 1361.

55. Freundlich, H. M. F. J. *Phys. Chem.* **1906**, *57*, 385.